ARTICLES

Diffusion and Structure of Water in Polymers Containing *N*-Vinyl-2-pyrrolidone

Ling-Shu Wan, Xiao-Jun Huang, and Zhi-Kang Xu*

Institute of Polymer Science and Key Laboratory of Macromolecule Synthesis and Functionalization (Ministry of Education), Zhejiang University, Hangzhou 310027, China

Received: August 9, 2006; In Final Form: November 22, 2006

Poly(*N*-vinyl-2-pyrrolidone) (PVP), a water-soluble polymer, is known for its excellent biocompatibility. It is generally recognized that the properties of polymers may be profoundly affected by the structure of water absorbed in them. In this study, Fourier transform infrared (FT-IR) in attenuated total reflection (ATR) and transmission mode was performed to examine the diffusion and structure of water in PVP and its copolymers. The obtained spectra were analyzed using two-dimensional (2D) IR with the aid of density functional theory (DFT) calculations. The 2D IR of time-resolved FT-IR/ATR spectra shows that type II water between 3300 and 3500 cm^{-1} occurs earlier during the water absorption process, which is also demonstrated by transmission FT-IR at the initial stage of water absorption. Conversely, type II water changes last when desorption takes place. Results from DFT calculations indicate that type II water might be monomeric or dimeric water molecules interacting with a carbonyl group in the pyrrolidone moiety. Furthermore, it is found that vibrations less than 3300 cm^{-1} (type I water) arise from water molecules involved in a carbonyl group interacting with more than two water molecules. It is reasonable that the transmission FT-IR spectra of film with an extra low water amount hardly show vibration bands below 3300 cm^{-1}; however, this region is distinct in the FT-IR/ATR spectra of fully swollen film. In addition, vibration bands between 3800 and 3500 cm^{-1} (type III water) are assigned to free water or water with relatively weak hydrogen bonding, as supported by the transmission FT-IR spectra of polyacrylonitrile (PAN) and the calculation results. Therefore, the diffusion process and the structures of water in PVP and its copolymers can be successfully accessed on the basis of the 2D IR analysis and DFT calculations.

Introduction

Water, one of the simplest and most important molecules, has great effects on the properties of polymers. The diffusion behaviors and states of water in epoxy resins, which have been used in numerous industrial fields, have received considerable interest because the absorbed water shows detrimental effects on the physical properties of the materials. Remarkable progress in this area has been achieved owing to lots of excellent work performed by Musto,[1−3] Sung,[4] Wu,[5] Li,[5−7] Maréchal,[8] and their co-workers.

Here, we concentrate on the absorption, states, and effects of water in polymers for biomedical applications. Biocompatibility is one of the major concerns while developing biomedical polymers. It is generally recognized that, when a synthetic polymer comes into contact with a living body, water absorption is the first event before protein adsorption. Therefore, some researchers have suggested that the absorbed water layer on the polymer surface determines all further events.[9−13] In other words, the existence of water on a polymer surface and its states may affect or even determine the biocompatibility of the polymer.

Vogler reviewed the structure and reactivity of water at biomaterial surfaces from the point of molecular self-association.[10] He concluded that there are at least two distinct kinds of water structure and reactivity, that is, a relatively less-dense water region against hydrophobic surfaces with an open hydrogen-bonded network and a relatively more-dense water region against hydrophilic surfaces with a collapsed hydrogen-bonded network. Kitano and Tanaka et al.[13−16] studied the structure of water absorbed in poly(2-methoxyethyl acrylate) (PMEA), which is of excellent blood compatibility, and its copolymers as well as the analogous polymers by Fourier transform infrared (FT-IR) spectroscopy, thermal analysis, and calculations of vibrational frequencies. They suggested that the main factor causing the excellent blood compatibility of PMEA is freezing bound water, which prevents the blood components from contacting the polymer surface or nonfreezing water on the polymer surface. Recently, they also pointed out that the water in a thin film of PMEA has a similar hydrogen-bonded network structure to that of free water.[11,16] The corrected number of hydrogen bonding defects existing in the hydrogen-bonded network structure of water per monomer unit of a polymer, N_{corr}, was proposed on the basis of Raman spectroscopy to elucidate the perturbation induced by polymer segments. Polymers having both hydrophilic and hydrophobic moieties, for example, poly(ethylene glycol) (PEG) and poly(*N*-vinyl-2-pyrrolidone) (PVP), often show a very small N_{corr} value, because ionized or polar groups may disturb the hydrogen bonding between water

* Corresponding author. Fax: + 86 571 8795 1773. E-mail: xuzk@zju.edu.cn.

10.1021/jp065152g CCC: $37.00
Published on Web 01/11/2007

molecules and raise the N_{corr} value while hydrophobic moieties such as hydrocarbon chains may enhance the hydrogen bonding and reduce the N_{corr} value. The resistance to protein adsorption of PEG has also been examined by many research groups. Kreuzer and Grunze et al.[12,17] published their results from calculations which demonstrated that the stability of a water interface with helical PEG chains prevents proteins and other macromolecules from directly contacting a PEG surface.

It seems that these findings sometimes are inconsistent with each other, which might be due to the fact that the absorption of water in polymers as well as its states is very complex. Therefore, many techniques have been applied to study the interactions of water with polymers, which include Fourier transform infrared (FT-IR),[1,6,8,11,15,18−23] Raman,[11] ultraviolet (UV),[4] nuclear magnetic resonance (NMR),[24] dielectric relaxation spectroscopy,[23] fluorescence spectroscopy,[20] thermal analysis,[9,13,21] and calculations.[11,15,23,25] Among these techniques, FT-IR shows some attractive advantages. Such spectroscopic methods provide information relating to structures and processes on a picosecond time scale (10^{-10}−10^{-15} s) and are more general and more sensitive than diffraction methods, and so forth. They can be commonly used to identify the presence of hydrogen bonding in all states of matter.[26] Furthermore, generalized two-dimensional (2D) correlation FT-IR spectroscopy, proposed by Noda,[27,28] has been developed to analyze various types of spectral data, which not only enhances the spectral resolution of highly overlapped FT-IR bands but also provides the specific sequence of spectral intensity changes.

Unlike PEG, PVP and its copolymers have not gotten enough attention, though this type of polymer is also of excellent biocompatibility. It is well-known that PVP has been widely used as an additive for the fabrication of polymeric membranes and profoundly enhances the blood compatibility and/or antifouling ability of the membranes.[29,30] Chemical modification with PVP on polysulfone or polyurethane has also been reported to improve their blood compatibility.[31,32] Sakai et al. revealed the morphology of PVP on polysulfone membranes using atomic force microscopy, and then, the blood compatibility was related to the surface particles formed by PVP, which produced a smooth surface after being swelled.[29,30] Nevertheless, interactions with water molecules of PVP remain to be further understood. Our previous research has confirmed the excellent biocompatibility of poly[acrylonitrile-*co*-(*N*-vinyl-2-pyrrolidone)].[33,34] The swelling behavior and the states of water have been investigated for these copolymers. It was found from the results of thermal analysis that the amounts of both free water and nonfreezable bound water increased remarkably with the content of *N*-vinyl-2-pyrrolidone (NVP). However, thermally analysis cannot give evidence for the interactions of water with the NVP moiety and the structure of water from a molecular level. In this work, therefore, to elucidate the interactions between water molecules and PVP (or its copolymers) from a molecular level, FT-IR spectra in attenuated total reflection (ATR) mode and transmission mode were therefore analyzed using 2D correlation techniques and then were related to the results of density functional theory (DFT) calculations.

Experimental Section

Materials. Poly(*N*-vinyl-2-pyrrolidone) (PVP, K90, $M_r \sim$ 360 000 g/mol) was purchased from Fluka and used as received. Polyacrylonitrile (PAN) and poly[acrylonitrile-*co*-(*N*-vinyl-2-pyrrolidone)] (PANCNVP) were synthesized in our laboratory by the solution polymerization method. Details for the characterization of the polymers were described in our previous papers.[33,34] PANCNVPs with 7, 15, and 22 wt % *N*-vinyl-2-pyrrolidone (NVP) were used in this work. Chloroform ($CHCl_3$) and *N*,*N*-dimethylformamide (DMF) were commercially obtained from Shanghai Chemical Agent Co. (China) and purified according to normal procedures before use. Ultrapure water (18.2 MΩ·cm) was used for all water absorption measurements.

Time-Resolved FT-IR/ATR. The film samples used for ATR measurements were cast from PANCNVP22 solution by solvent evaporation in a vacuum at 80 °C. The thickness of the film was approximately 18 ± 2 μm. Time-resolved FT-IR/ATR measurements were performed using a Nicolet FT-IR/Nexus470 spectrometer equipped with an ATR accessory (ZnSe crystal, 45°). All spectra were taken by 16 scans at a nominal resolution of 4 cm^{-1}. The film-covered ATR crystal with a filter paper above the sample film was mounted in an ATR cell, and the spectra of the dry film were collected as background spectra; then, without moving the sample, distilled water was injected into the filter paper while starting the data acquisition. The relative humidity (RH) of air was kept at about 70% (25 °C). To observe the water-desorbing process, the wet filter paper was replaced by a dry one and then the spectra were collected. A typical absorbing/desorbing loop lasted 50−60 min, and the acquisition time interval was 70 s. The absorbed water in PANCNVP film can be determined by weighing the film before and after the measurements. Thus, the number of water molecules per NVP unit can be obtained for the polymer containing 22 wt % NVP units.

Transmission FT-IR. Before the measurements of transmission FT-IR for PAN and PANCNVP22, these polymers were dissolved in DMF, coated on a calcium fluoride (CaF_2) salt plate, and dried in vacuum at 80 °C to remove the solvent completely. To investigate the water absorbed into the polymer with different NVP contents, the salt plate covered with polymer film stayed in the atmosphere (25 °C, 70% RH) for 10 min after being taken out of the vacuum oven. Afterward, FT-IR spectra (or time-resolved spectra) were collected with a resolution of 4 cm^{-1} and eight scans.

PVP K90 was dissolved in chloroform to form a 1 wt % homogeneous solution. The solution was coated on a dry sodium chloride (NaCl) salt plate, and then, FT-IR spectra were collected immediately with a resolution of 4 cm^{-1} and eight scans. Measurements were carried out in the atmosphere (25 °C, 70% RH). A typical sorption loop lasted 20 min, and the acquisition time interval was 120 s.

2D Correlation Analysis. At least 10 spectra at different times in certain wavenumber ranges were selected for 2D correlation analysis using the software (2Dshige (c) Shigeaki Morita, Kwansei-Gakuin University, 2004−2005). In the 2D correlation maps, unshaded regions indicate positive correlation intensities, while shaded regions indicate negative correlation intensities.

Computational Methods. As the model compounds, various combination numbers of water and polymer units were used. Molecular geometries of the model compounds were optimized and followed by the frequency calculation using a hybrid density functional method, Becke3LYP (B3LYP) with a 6-31++G(d,p) basis set. Recently, the B3LYP exchange-correlation method has been widely used to obtain the frequency of a number of molecular systems.[11,25] All of the calculations were carried out using a Gaussian 98 program package.[35] The deviation from the experimental frequency was generally found even for a single water molecule, when we employed larger basis sets and more accurate correlation. Our object is, however, the assignment of the experimental O−H stretching bands with the help

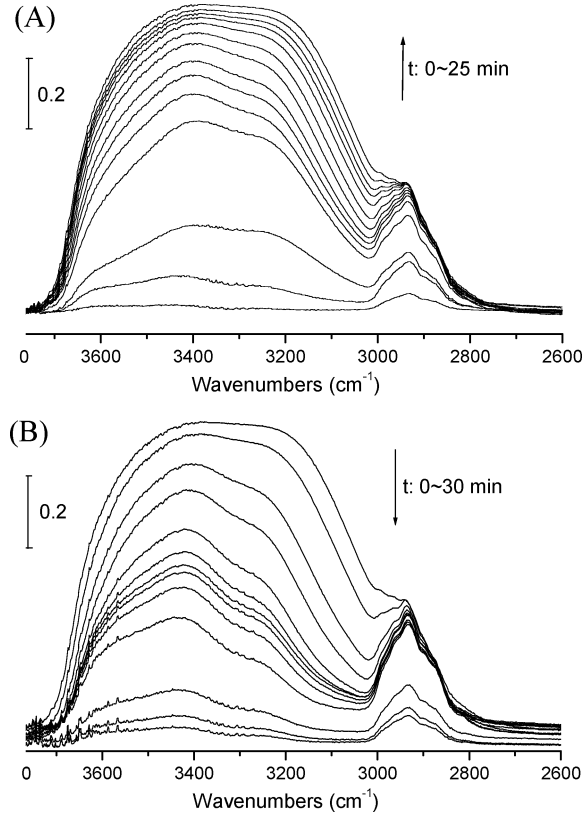

Figure 1. Temporal changes of FT-IR/ATR spectra in the wavenumber range 3800−2800 cm^{-1} during the (A) water-absorbing and (B) water-desorbing processes of PANCNVP film. The measurements were performed at 25 °C and about 70% RH.

of the theoretical frequency of the model compounds. Therefore, theoretical frequencies from the B3LYP/6-31++G(d,p) calculations were corrected using a shift parameter in the present study, and the shift parameter was determined as 0.9584.

Results and Discussion

Water Diffusion Measurements by Time-Resolved FT-IR/ATR. It is well-known that the fundamental stretching vibrations and the in-plane bending of water occur within the 3800−2800 cm^{-1} region and that around 1640 cm^{-1} (ν_2). In our case, the discussion followed will be focused on the 3800−2800 cm^{-1} wavenumber region, where the peaks are considerably more intense. Besides, it has been proved that more information about the hydrogen bonding can be obtained from the analysis of the wavenumber region characteristic of the O−H stretching vibrations.[1] Thus, the water vibration bands at 3800−2800 cm^{-1}, for the water-absorbing and -desorbing processes, are shown in parts A and B of Figure 1, respectively.

As we know, the FT-IR/ATR spectrum provides information of water located in polymer film with a certain depth. The penetration depth, d_p, of FT-IR/ATR at 3000 cm^{-1} is about 0.66 μm according to the following equation:

$$d_p = \lambda_1/[2\pi(\sin^2\theta - n_{21}^2)^{1/2}]$$

where θ is the incident angle of light on the surface of the ATR crystal, λ_1 is the ratio of the wavelength of incident light to the refractive index of the ATR crystal, and n_{21} is the ratio of the refractive index of the polymer to that of the ATR crystal. Therefore, in our case, only water in the film surface layer near the ATR crystal side is detected for the thickness of film is about 18 μm, which is far larger than the d_p value (~0.66 μm).

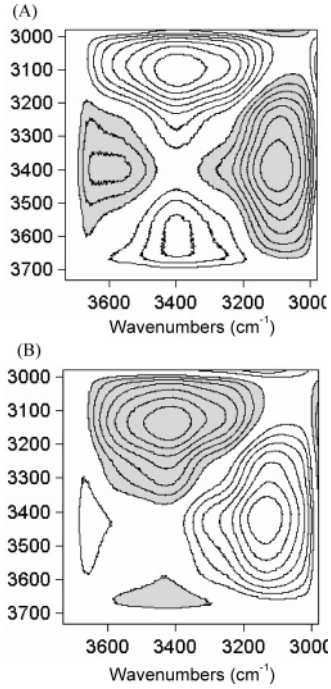

Figure 2. Asynchronous 2D IR correlation spectra in the wavenumber range 3700−3000 cm^{-1}. Parts A and B were obtained from the time-resolved FT-IR/ATR spectra of the water-absorbing and water-desorbing processes, respectively.

As shown in Figure 1, the vibration bands in this region are overlapped to a broad peak. It is found that the band around 2900 cm^{-1}, which is mainly due to the stretching vibration of C−H bonds, monotonously increases in the water absorption process. The swelling of polymer film will decrease its refractive index and the fraction of C−H bonds in the detectable depth. Therefore, the intensity of the band should decrease in this process. However, the result is contrary to expectation. Similar phenomena have also been reported, and no explanation was given.[5] Although it is still ambiguous to some extent, it is speculated that the increase may be attributed to the overlap with the hydrogen bond region. For the isolated water molecule in the gas phase, there are three distinct peaks in the O−H stretching region, centered at 3652 cm^{-1} (ν_1, symmetric stretching), 3756 cm^{-1} (ν_3, antisymmetric stretching), and 3151 cm^{-1} ($2\nu_2$). For the structure of liquid water, however, there is still something conflicting. Curve-fitting analysis is often performed to resolve the overlapped peak for a quantitative assessment of water species with the aid of deconvoluted and second-derivative spectra. Recently, 2D correlation analysis has advanced as a powerful tool. Figure 2 shows the 2D asynchronous correlation spectra of the water absorbed in PANCNVP22 film in the spectral range 3800−3000 cm^{-1}. The appearance of an asynchronous cross-peak, $\Psi(\nu_1/\nu_2)$, indicates that the bands ν_1 and ν_2 vary out of phase with each other during the diffusion process.[27,28] One negative cross-peak (3628/3398 cm^{-1}) and one positive cross-peak (3398/3097 cm^{-1}) observed in Figure 2A (water absorption process) indicate that the broad ν(O−H) water band in the spectral range 3800−3000 cm^{-1} is clearly split into three separate bands located at 3628, 3398, and 3097 cm^{-1}. Similarly, three separate bands located at 3657, 3424, and 3135 cm^{-1} can be observed for the water-desorbing process (Figure 2B). The sign of the cross-peak in an asynchronous spectrum provides additional information about the order of the intensity changes in different bands. According to the rule of Noda,[27,28] during the process of water absorption (Figure 2A), the band at 3398 cm^{-1} varies prior to those at 3097 and 3628

cm^{-1}. On the contrary, for the process of water desorption (Figure 2B), the band at 3424 cm^{-1} changes after those at 3135 and 3657 cm^{-1}.

To elucidate the diffusion behavior of water and its structure in polymer film, assignments of these bands must be made. Several models have been proposed. For example, water in polymers has been classified into water with strong hydrogen bonding (type I water, hereafter), water with moderately strong hydrogen bonding (type II water, hereafter), and water without hydrogen bonding or with weak hydrogen bonding (free water or type III water, hereafter).[36] More simply, bound water and free water have also been assigned.[7] In our case, the change of type II water (3398 cm^{-1}) occurs earlier than those of type I water (3097 cm^{-1}) and type III water (3628 cm^{-1}) for the water absorption process. It means that water molecules contacting polymer film preferentially form moderately strong hydrogen bonding (or other unknown species) followed by the formation of strongly bound water and free water.[36] During the water absorption process, as shown in Figure 2B, the intensity of cross-peak 3657/3424 cm^{-1} is very small, while that of cross-peak 3424/3135 cm^{-1} is very large, which is derivable from Figure 1B that the intensity at a low wavenumber region decreases fast. Though type III water (3657 cm^{-1}) is easy to be desorbed, it may be reasonable because the type I water (3135 cm^{-1}) and type II water (3424 cm^{-1}) may dissociate or weaken into type III water. In addition, it should be noted that all three split bands for the water-desorbing process locate at larger wavenumber regions than those for the water absorption process, which indicates the decrease of hydrogen bonding strength and a looser hydrogen bonding structure due to the driving force of dehydration.

It seems that the water diffusion process can be analyzed by 2D IR soundly. However, at least two issues still remain: (1) The ATR spectra correspond to almost fully swollen film, as can be seen from the absorption shown in Figure 1. Thus, is it certain that type II water changes first during the water absorption process? (2) What is the possible structure of each type of water in the studied polymer film? To this end, transmission FT-IR monitoring the water absorption at the initial stage and preliminary vibrational frequency calculations were performed.

Transmission FT-IR of PVP and Its Copolymers. It is well-known that transmission FT-IR examines the bulk of polymer film while FT-IR/ATR only detects the surface. The surface and bulk structure/property are different for PAN and PANCNVP. However, it is generally accepted that surface reconstruction is remarkable only for block copolymer or comb copolymer.[37,38] In our cases, PANCNVP is a random copolymer, and thus, the effects of the difference between surface/bulk on the FT-IR results may be ignored.

To obtain a "completely dry" polymer film layer, the CaF_2 salt plate coated with polymer solution was promptly transferred into a vacuum oven after the coating. Then, the salt plate was placed into the spectrometer cell for measurements after the solvent was entirely removed. If we start the measurements immediately, there is no absorption for all polymer films in the spectral range 3800−3000 cm^{-1}. Thus, the sample stayed in the atmosphere (25 °C, 70% RH) for 10 min before spectra collection. Figure 3 shows the FT-IR transmission spectra of polymers with different NVP contents.

It can be seen that the absorption increases remarkably with the content of NVP in the polymer. It is well-known that PVP is water-soluble and can be used as a hydrogel material, which may be attributed to the hydrophilic carbonyl group in the pyrrole ring. Furthermore, polymers with a higher content of NVP, especially PANCNVP22 (Figure 3d), show a sharp peak around 3341 cm^{-1}. This peak just belongs to the region of type II water, as mentioned above.

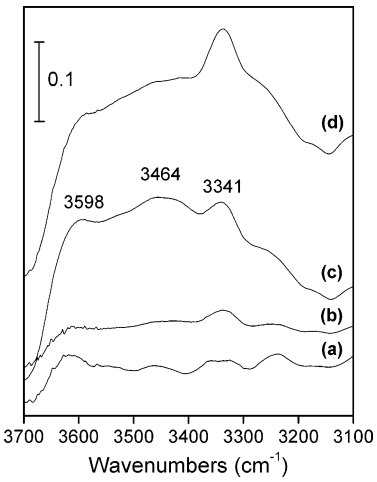

Figure 3. FT-IR transmission spectra of polymers coated on a calcium fluoride salt plate. The content of NVP in the polymers is (a) 0%, (b) 7%, (c) 15%, and (d) 22%. Measurements were performed after the polymer-coated salt plate was transferred from the vacuum oven to the FT-IR cell and exposed to air with a 70% RH at 25 °C for 10 min.

Transmission FT-IR spectra of pure PVP were also collected with time to further confirm the water absorption at the initial stage. Different from the PANCNVP films, PVP film coated from $CHCl_3$ solution absorbs water fast and tightly, and some bound water cannot be removed. As shown in Figure 4A, a small peak around 3341 cm^{-1}, which also is equal to the sharp peak showed in PANCNVP transmission FT-IR spectra, can be observed even for the first scan. In other words, the stretching vibrational frequency of water initially bound with PVP is truly located at about 3341 cm^{-1}. Therefore, in view of the fact that the transmission IR provides information at the initial stage of water absorption in our cases, it is proved that type II water is formed first during the water absorption process, as analyzed by 2D IR. In addition, the region around 3470 cm^{-1} might be assigned to the type II water, while that around 3550 cm^{-1} might be attributed to free water. In Figure 4B, the peak at 1681.5 cm^{-1}, the vibration band arising from the carbonyl group in NVP, obviously shifts to 1669.5 cm^{-1} after water absorption. This red shift also indicates the interactions between water molecules and the carbonyl groups.

Time-resolved transmission FT-IR spectroscopy was performed to observe the PAN and PANCNVP films with lower water content. It can be seen from Figure 5 that PANCNVP obviously absorbs more water than PAN in the given time. Moreover, PAN shows only a sharp peak around 3625 cm^{-1}, while PANCNVP shows a broad peak in the range 3650−3250 cm^{-1}. This difference indicates that PAN really only gives rise to type III water; in other words, type III is really caused by free water or water with weak hydrogen bonding. On the contrary, similar to Figure 3d, the spectra in Figure 5B show several overlapped peaks, such as those around 3341 and 3470 cm^{-1}, which may be mainly attributed to the water molecules interacting with NVP moieties.

The results of 2D correlation analysis of the above-mentioned time-resolved transmission FT-IR spectra are shown in Figure 6. The asynchronous 2D IR spectrum for PAN (Figure 6A) reveals many small cross-peaks, which are mostly found around 3600 cm^{-1}. For PANCNVP, as shown in Figure 6B, one negative cross-peak (3472/3341 cm^{-1}) and one positive cross-

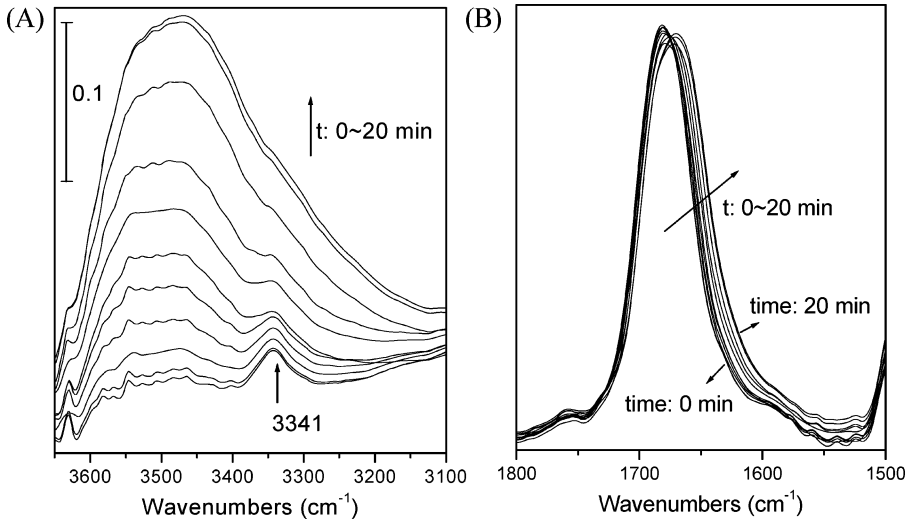

Figure 4. Temporal changes of FT-IR transmission spectra in the wavenumber ranges (A) 3700−3100 cm^{-1} and (B) 1800−1500 cm^{-1} of PVP. The PVP K90 solution was coated on a sodium chloride (NaCl) salt plate and dried. The dried PVP-coated salt plate was then exposed to air with a 70% RH at 25 °C, and the spectra were collected with time.

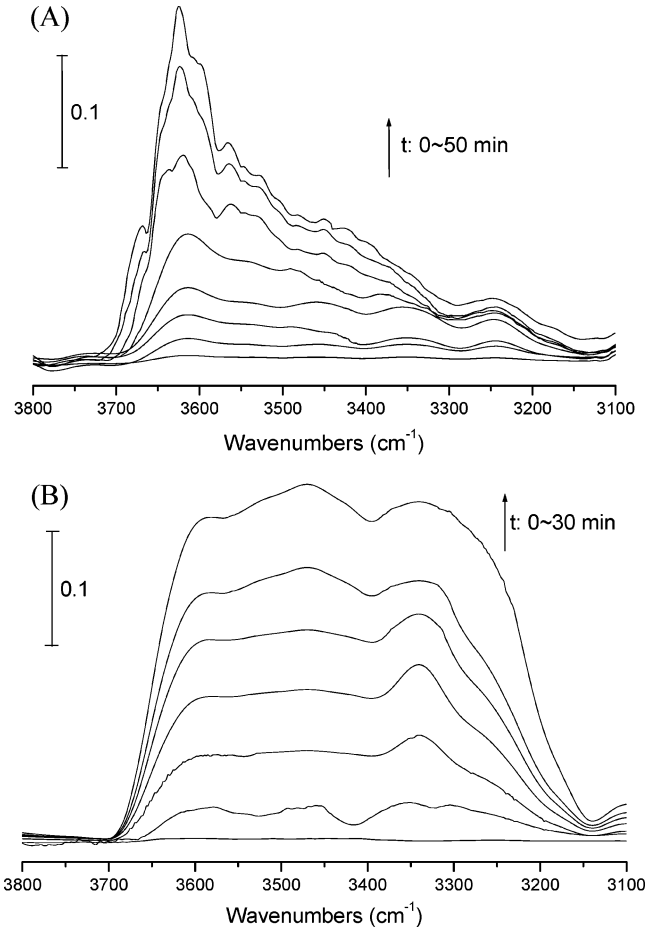

Figure 5. Temporal changes of FT-IR transmission spectra in the wavenumber range 3800−3100 cm^{-1} of (A) PAN and (B) PANCNVP22. The polymer solution was coated on a CaF_2 salt plate and dried in a vacuum oven. The dry polymer-coated salt plate was then exposed to air with a 70% RH at 25 °C, and the spectra were collected with time.

peak (3341/3243 cm^{-1}) can be observed. Peaks at 3472 and 3341 cm^{-1} belong to the type II water, while that at 3243 cm^{-1} can be assigned to the type I water. Besides, it can be induced that the peak at 3341 cm^{-1} varied prior to those at 3472 and 3243 cm^{-1}.

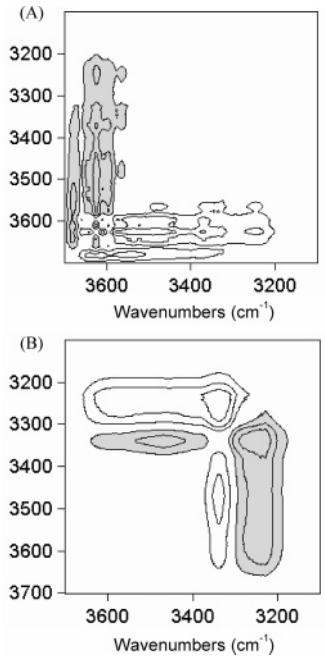

Figure 6. Asynchronous 2D IR correlation spectra in the wavenumber range 3700−3100 cm^{-1}. Parts A and B were obtained from the time-resolved transmission spectra of (A) PAN and (B) PANCNVP22 coated on a CaF_2 salt plate, respectively.

Calculated Vibrational Frequencies. Knowledge of the molecular structure for each water species in polymer may be important to understand the effects of absorbed water. For example, the structures of water surrounding a polymer segment may profoundly affect the contact of biomacromolecules with the polymer surface.[12] Except for the classification of water structure according to the strength of hydrogen bonding, the structure of water was described in terms of a relatively small number of discrete species, such as three spectroscopically distinguishable species designated as S_0, S_1, and S_2, where the subscripts denote the number of hydrogen atoms of the water molecule involved in hydrogen bonding. On the basis of this model, subpeaks from curve-fitting analysis were identified for an epoxy resin system by Musto et al.[1] Kitano et al. also obtained a number of subpeaks in the spectral range 3800−3000 cm^{-1} by curve-fitting analysis. Also, these subpeaks were

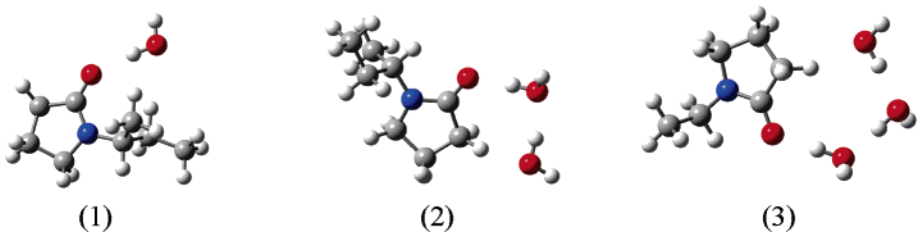

Figure 7. Optimized structures of the NVP unit interacting with water molecules.

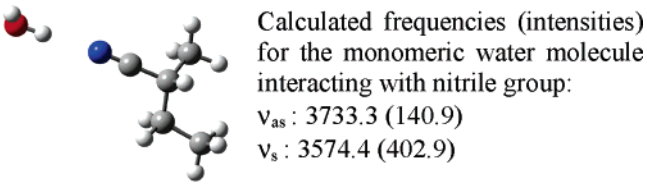

Figure 8. Optimized structure and the calculated frequencies (intensities) for the monomeric water molecule interacting with a nitrile group.

TABLE 1: Calculated IR Frequencies and Intensities of Hydrogen Bonding for the Hydrating Model Compounds

		frequency[a]		intensity	
No.	model compound	ν_{as}	ν_{s}	$I\nu_{as}$	$I\nu_{s}$
0	HOH	3763.8	3646.4	53.7	5.0
1	−CO−HOH	3729.1	3478.1	94.6	576.6
2	−CO−***HOH***−HOH	3723.0	**3267.2**	81.5	**1222.4**
	−CO−HOH−***HOH***	3726.3	**3382.6**	55.5	**566.3**
3	−CO−***HOH***−HOH−HOH	3729.4	**3222.1**	86.0	**1448.2**
	−CO−HOH−***HOH***−HOH	3722.2	3299.7	66.5	934.0
	−CO−HOH−HOH−***HOH***	3725.5	3371.1	52.3	535.7

[a] co = 0.9584.

assigned by combining IR vibrational frequency calculations from different hydrating model compounds. Recently, the B3LYP method has been widely used to obtain the frequency of a number of molecular systems.[11,39] We report here preliminary results from the calculations of some hydrating model compounds designed to assess the assignments of water in PANCNVP. The optimized structures for NVP and acrylonitrile (AN) units are shown in Figures 7 and 8, respectively. The calculated IR frequencies and intensities of hydrogen bonding are summarized in Table 1 in which the serial numbers (No.) correspond to those in Figure 7.

It is clear that the calculated intensity of the symmetric stretching vibration (ν_s) for hydrating water is much larger than that of the antisymmetric one (ν_{as}) in almost all cases except for that of a separate water molecule. For example, the intensity ratio of ν_s to ν_{as} for the compound 1 (C═O···HOH) is about 6.1:1.0. Only ν_s is therefore considered for the assignments.[15,25] Vibrational bands at a high wavenumber region, such as 3800−3500 cm^{-1}, often originate from free water or water with relatively weak hydrogen bonding (type III water). As shown in Figure 8, the calculated frequency of model compound AN (CN···HOH) is high to 3574 cm^{-1}; besides, the ratio of ν_s to ν_{as} is only about 2.9. Hence, free water and water with relatively weak hydrogen bonding such as water interacting with a nitrile group cause the vibration between 3800 and 3500 cm^{-1}, which can be confirmed by the spectra of PAN shown in Figure 5. The frequencies between 3300 and 3500 cm^{-1} belonging to the type II water might be due to the monomeric or dimeric water molecules interacting with a carbonyl group (compounds 1 and 2). Meanwhile, the frequencies below 3300 cm^{-1} should be attributed to the water molecules involved in a carbonyl group interacting with more than two water molecules such as compound 3 (C═O···*HOH*···HOH···HOH), which correspond to the type I water. This type of water is largely found in Figure 1 due to the fully swollen PANCNVP film. In our cases, the results of gravimetry confirm that the absorbed water is about 0.34 g of water/g of dry film after ATR measurements, which means one NVP unit may occupy up to 9.5 water molecules. Therefore, the NVP unit during ATR measurement may bind three or more than three water molecules though the nitrile groups and the free volume holes in the film would occupy some of the water. It was also reported that one NVP unit could bind at least 4.2 water molecules on the basis of the results of thermal analysis.[40,41] Furthermore, type I water is hardly found in Figures 3 and 4. For example, the bands below 3300 cm^{-1} are very weak in Figure 4 because the absorbed water is little at the initial stage. Therefore, it is possible that the bands below 3300 cm^{-1} come from the three or more than three water molecules (type I water) bound with one NVP unit.

On the basis of the assigned structures, the preferential formation of type II water (compound 2) indicated by the 2D IR spectra may benefit the water diffusion at the initial stage of water absorption. Some researchers suggested that water molecules first occupied free volume holes and then bound to specific chain segments or groups; however, other researchers proposed that water molecules migrated through the bulk of the polymer network via jumping motions from one site to another.[1,2,7,24] It is speculated that, in the dimeric water (C═O···HOH···HOH), the water molecule bridging carbonyl group and the other water molecule may transport the latter (this water molecule has only one hydrogen bond and is ready to form another hydrogen bond) from one site to another.

In addition, the monomeric water molecule interacting with a carbonyl group may also be assigned to type II water. Compound 1, in which one water molecule is interacting with a carbonyl group, induces the vibration band around 3478 cm^{-1}. Figures 3, 4, and 5B show a distinct peak at around 3341 cm^{-1} as well as a broad band within the region 3400−3500 cm^{-1}. Figure 6B also reveals a peak at about 3478 cm^{-1}. Considering the very low content of absorbed water during these transmission IR measurements, one water molecule occupying a carbonyl group may be reasonable.[15]

Conclusion

FT-IR in attenuated total reflection and transmission mode was performed to examine the diffusion and structure of water in PVP and its copolymers. The obtained spectra were analyzed using 2D IR with the aid of DFT calculations. It is proved that, during the water absorption process, type II water between 3300 and 3500 cm^{-1} is first formed followed by type I water (less than 3300 cm^{-1}) and type III water (3800−3500 cm^{-1}). Transmission FT-IR at the initial stage of water absorption also demonstrates type II water. Conversely, type II water changes last when desorption takes place. Results from DFT calculation indicate that type II water might be monomeric or dimeric water molecules interacting with a carbonyl group. It is also found that vibrations less than 3300 cm^{-1} (type I water) arise from

water molecules involved in a carbonyl group interacting with more than two water molecules, which is confirmed by the fact that the transmission FT-IR spectra of PVP or PANCNVP22 film with an extra low water amount hardly show vibration bands below 3300 cm^{-1}, while this band is remarkable in FT-IR/ATR spectra of a fully swollen polymer film. Furthermore, the vibration bands around 3478 cm^{-1} shown in both FT-IR/ATR and transmission spectra are attributed to the water molecules involved in a water molecule occupied one carbonyl group. In addition, vibration bands between 3800 and 3500 cm^{-1} are assigned to free water or water with relatively weak hydrogen bonding according to the calculations, as supported by the transmission FT-IR spectra of PAN. In conclusion, the strongly bound water of PVP may be responsible for its good biocompatibility.

Acknowledgment. Financial support from the National Natural Science Foundation of China for Distinguished Young Scholars (Grant No. 50625309) is gratefully acknowledged.

References and Notes

(1) Musto, P.; Ragosta, G.; Mascia, L. *Chem. Mater.* **2000**, *12*, 1331.
(2) Cotugno, S.; Mensitieri, G.; Musto, P.; Sanguigno, L. *Macromolecules* **2005**, *38*, 801.
(3) Cotugno, S.; Larobina, D.; Mensitieri, G.; Musto, P.; Ragosta, G. *Polymer* **2001**, *42*, 6431.
(4) Weir, M. D.; Bastide, C.; Sung, C. S. P. *Macromolecules* **2001**, *34*, 4923.
(5) Liu, M. J.; Wu, P. Y.; Ding, Y. F.; Chen, G.; Li, S. J. *Macromolecules* **2002**, *35*, 5500.
(6) Li, L.; Liu, M. J.; Li, S. J. *J. Phys. Chem. B* **2004**, *108*, 4601.
(7) Li, L. N.; Zhang, S. Y.; Chen, Y. H.; Liu, M. J.; Ding, Y. F.; Luo, X. W.; Pu, Z.; Zhou, W. F.; Li, S. J. *Chem. Mater.* **2005**, *17*, 839.
(8) Ngono, Y.; Marechal, Y.; Mermilliod, N. *J. Phys. Chem. B* **1999**, *103*, 4979.
(9) Tanaka, M.; Mochizuki, A.; Ishii, N.; Motomura, T.; Hatakeyama, T. *Biomacromolecules* **2002**, *3*, 36.
(10) Vogler, E. A. *Adv. Colloid Interface Sci.* **1998**, *74*, 69.
(11) Kitano, H.; Tada, S.; Mori, T.; Takaha, K.; Gemmei-Ide, M.; Tanaka, M.; Fukuda, M.; Yokoyama, Y. *Langmuir* **2005**, *21*, 11932.
(12) Wang, R. L. C.; Kreuzer, H. J.; Grunze, M. *J. Phys. Chem. B* **1997**, *101*, 9767.
(13) Tanaka, M.; Mochizuki, A. *J. Biomed. Mater. Res. Part A* **2004**, *68A*, 684.
(14) Kitano, H.; Ichikawa, K.; Fukuda, M.; Mochizuki, A.; Tanaka, M. *J. Colloid Interface Sci.* **2001**, *242*, 133.
(15) Ichikawa, K.; Mori, T.; Kitano, H.; Fukuda, M.; Mochizuki, A.; Tanaka, M. *J. Polym. Sci., Part B: Polym. Phys.* **2001**, *39*, 2175.
(16) Ide, M.; Mori, T.; Ichikawa, K.; Kitano, H.; Tanaka, M.; Mochizuki, A.; Oshiyama, H.; Mizuno, W. *Langmuir* **2003**, *19*, 429.
(17) Schwendel, D.; Dahint, R.; Herrwerth, S.; Schloerholz, M.; Eck, W.; Grunze, M. *Langmuir* **2001**, *17*, 5717.
(18) Gemmei-Ide, M.; Motonaga, T.; Kitano, H. *Langmuir* **2006**, *22*, 2422.
(19) Ide, M.; Yoshikawa, D.; Maeda, Y.; Kitano, H. *Langmuir* **1999**, *15*, 926.
(20) Thouvenin, M.; Linossier, I.; Sire, O.; Peron, J. J.; Vallee-Rehel, K. *Macromolecules* **2002**, *35*, 489.
(21) Wang, Y. Q.; Kawano, Y.; Aubuchon, S. R.; Palmer, R. A. *Macromolecules* **2003**, *36*, 1138.
(22) Sammon, C.; Mura, C.; Yarwood, J.; Everall, N.; Swart, R.; Hodge, D. *J. Phys. Chem. B* **1998**, *102*, 3402.
(23) Mijovic, J.; Zhang, H. *Macromolecules* **2003**, *36*, 1279.
(24) Jelinski, L. W.; Dumais, J. J.; Cholli, A. L.; Ellis, T. S.; Karasz, F. E. *Macromolecules* **1985**, *18*, 1091.
(25) Kitano, H.; Ichikawa, K.; Ide, I.; Fukuda, M.; Mizuno, W. *Langmuir* **2001**, *17*, 1889.
(26) Jeffrey, G. A. *An introduction to hydrogen bonding*; Oxford University Press: New York, 1997.
(27) Noda, I. *J. Am. Chem. Soc.* **1989**, *111*, 8116.
(28) Noda, I. *Appl. Spectrosc.* **1990**, *44*, 550.
(29) Hayama, M.; Yamamoto, K.; Kohori, F.; Uesaka, T.; Ueno, Y.; Sugaya, H.; Itagaki, I.; Sakai, K. *Biomaterials* **2004**, *25*, 1019.
(30) Hayama, M.; Yamamoto, K.; Kohori, F.; Sakai, K. *J. Membr. Sci.* **2004**, *234*, 41.
(31) Higuchi, A.; Shirano, K.; Harashima, M.; Yoon, B. O.; Hara, M.; Hattori, M.; Imamura, K. *Biomaterials* **2002**, *23*, 2659.
(32) Wetzels, G. M. R.; Koole, L. H. *Biomaterials* **1999**, *20*, 1879.
(33) Wan, L. S.; Xu, Z. K.; Huang, X. J.; Wang, Z. G.; Wang, H. L. *Polymer* **2005**, *46*, 7715.
(34) Wan, L. S.; Xu, Z. K.; Huang, X. J.; Wang, Z. G.; Ye, P. *Macromol. Biosci.* **2005**, *5*, 229.
(35) Frisch, M. J.; Trucks, G. W.; Schlegel, H. B.; Scuseria, G. E.; Robb, M. A.; Cheeseman, J. R.; Zakrzewski, V. G.; Montgomery, J. A., Jr.; Stratmann, R. E.; Burant, J. C.; Dapprich, S.; Millam, J. M.; Daniels, A. D.; Kudin, K. N.; Strain, M. C.; Farkas, O.; Tomasi, J.; Barone, V.; Cossi, M.; Cammi, R.; Mennucci, B.; Pomelli, C.; Adamo, C.; Clifford, S.; Ochterski, J.; Petersson, G. A.; Ayala, P. Y.; Cui, Q.; Morokuma, K.; Malick, D. K.; Rabuck, A. D.; Raghavachari, K.; Foresman, J. B.; Cioslowski, J.; Ortiz, J. V.; Stefanov, B. B.; Liu, G.; Liashenko, A.; Piskorz, P.; Komaromi, I.; Gomperts, R.; Martin, R. L.; Fox, D. J.; Keith, T.; Al-Laham, M. A.; Peng, C. Y.; Nanayakkara, A.; Gonzalez, C.; Challacombe, M.; Gill, P. M. W.; Johnson, B. G.; Chen, W.; Wong, M. W.; Andres, J. L.; Head-Gordon, M.; Replogle, E. S.; Pople, J. A. *Gaussian 98*, revision A.3; Gaussian, Inc.: Pittsburgh, PA, 1998.
(36) Shen, Y.; Wu, P. Y. *J. Phys. Chem. B* **2003**, *107*, 4224.
(37) Hester, J. F.; Banerjee, P.; Mayes, A. M. *Macromolecules* **1999**, *32*, 1643.
(38) Fasolka, M. J.; Mayes, A. M. *Ann. Rev. Mater. Res.* **2001**, *31*, 323.
(39) Xu, Z.; Li, H. R.; Wang, C. M.; Wu, T.; Han, S. J. *Chem. Phys. Lett.* **2004**, *394*, 405.
(40) Galin, J. C.; Galin, M. *J. Polym. Sci., Part B: Polym. Phys.* **1992**, *30*, 1103.
(41) Ping, Z. H.; Nguyen, Q. T.; Chen, S. M.; Zhou, J. Q.; Ding, Y. D. *Polymer* **2001**, *42*, 8461.